DOI: 10.1002/ejoc.201000847

Severe Energy Costs of Double Steric Interactions: Towards a Molecular Clamp

Kirill Nikitin,*[a] Conor Fleming,[a] Helge Müller-Bunz,[a] Yannick Ortin,[a] and Michael J. McGlinchey*[a]

Keywords: Rotational barrier / Steric hindrance / Strained molecules / Molecular machinery / Molecular devices

The factors determining the ease of rotation about carbon–carbon single bonds connecting two internally rigid fragments such as phenyl, indenyl, anthracenyl and triptycyl are analysed. The internal rotation barriers in these molecules have been estimated on the basis of kinetic data or variable-temperature NMR measurements, and the crystal structures have been analysed in terms of steric strain. Computer simulation of the internal rotation indicates that the estimated Closest Approach Distance, CAD, between sterically interacting atoms of the two interconnected fragments can be a helpful parameter for evaluating their rotational freedom, but must be used with caution. Thus, the barrier to rotation of a 3-indenyl moiety linked to the 9-position of anthracene is very high ($\Delta G^{\neq} \approx 25$ kcal mol^{-1}) compared to that in 3-indenyltriptycene ($\Delta G^{\neq} \approx 12$ kcal mol^{-1}) despite the fact that the nominal CADs in both cases are very similar. Moreover, dimeric 2-methylindenyl fragments linked by a single bond at the 3-position undergo relatively slow rotation ($\Delta G^{\neq} \approx 14$–15 kcal mol^{-1}) owing to the simultaneous close approach of two pairs of sterically interacting hydrogens. Although the rotational barrier for a 2-indenyl or phenyl moiety attached to the bridgehead atom of triptycene, or to the related dibenzobicyclo[2.2.2]octane system, is relatively low ($\Delta G^{\neq} \approx 8$–9 kcal mol^{-1}), further extension of the bridge to dibenzobicyclo[2.2.4]dioxadecane leads to an activation energy barrier in excess of 23 kcal mol^{-1}, attributable to an intramolecular simultaneous "clamping" of the phenyl rings by the edges of the aromatic rings of the dibenzobicyclo[2.2.4]dioxadecane moiety. The X-ray crystal structures of 15 molecules, including mono- and di-indenyl-anthracenes, *racemic*- and *meso*-2-methylindenyl dimers, phenyl- and indenyl-triptycenes and -barrelenes, are reported.

Introduction

Rotation about sp^3–sp^3 carbon–carbon single bonds in non-hindered molecules is very rapid at ambient temperature.[1] Hence, rotations in alkanes are normally too fast to be studied by dynamic NMR at room temperature since the barriers are less than 5 kcal mol^{-1}.[2] However, it has been demonstrated that, in appropriately substituted systems, rotation about single bonds linking two aromatic carbon atoms can be significantly slowed down, and even stopped on a chemically significant time-scale.[3,4] In these cases, barriers can exceed 25 kcal mol^{-1} and so open up the possibility of designing controlled molecular brakes, ratchets and other functional molecular systems.[5,6]

The key to the successful implementation of the proposed molecular design is the ability to tune the rotational barriers while maintaining the required molecular geometry and function. Particularly interesting as molecular building blocks are the substituted triptycenes[6a] and their structural analogues whereby C(9), a bridgehead tetrahedral carbon of the three-bladed paddlewheel, is linked to another rigid moiety, as in the examples depicted in Scheme 1. Since the rotation of the paddlewheel is typically hindered by steric repulsion between hydrogen atoms, or other molecular fragments proximate to the central carbon–carbon single bond, control of the barrier height may be achieved by structural modification, including functional group transformation or isomerisation. Another appealing structural class includes flat polycyclic aromatic hydrocarbon systems that also possess tetrahedral carbon centres. Importantly, such structures, e.g. indene or fluorene, can be readily converted into π complexed transition metal derivatives that undergo reversible haptotropic rearrangements involving a shuttle-like translational movement of the metal fragment.[7]

We have recently reported the syntheses and dynamic behaviour of two isomers, 9-(3-indenyl)triptycene (**1a**) and 9-(2-indenyl)triptycene (**1b**) in which the originally D_{3h}-symmetric triptycene is connected to the mirror-symmetric indene via an sp^3–sp^2 carbon–carbon single bond. Variable-temperature NMR studies revealed that, while the rotational barrier, $\Delta G^{\neq}$, in **1a** is 12 kcal mol^{-1}, rotation in **1b** is still fast on the NMR time-scale at –80 °C, suggesting a barrier no greater than 8 kcal mol^{-1}.[8]

The complex interplay of factors determining rotational barriers in a wide range of molecules is a fundamental topic in modern organic chemistry,[9] and a better understanding of such processes would be valuable for the design of components in molecular machinery. For example, in a very recent paper we described how the low-barrier system **1b**

[a] School of Chemistry & Chemical Biology University College Dublin,
Belfield, Dublin 4, Ireland
Fax: +353-1-716-1178
E-mail: kirill.nikitin@ucd.ie
michael.mcglinchey@ucd.ie

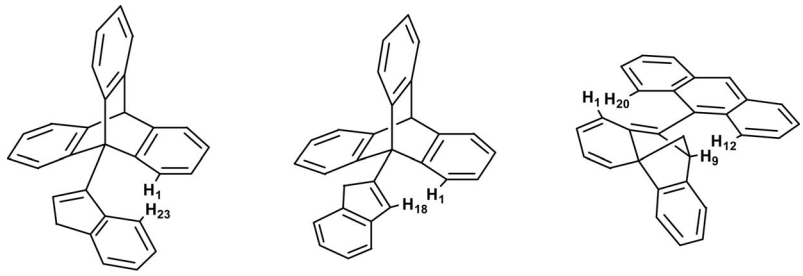

1a 1b 1c

Scheme 1. Potential steric clashes and rotational barriers in indenyltriptycenes **1a** (12 kcal mol^{-1}), **1b** (<8 kcal mol^{-1}), and in the isomeric methanophenanthrenyl-anthracene derivative **1c** (>18 kcal mol^{-1}).

could be modified by complexation to the indenyl of a π-bonded tricarbonylchromium moiety to work as the first haptotropically-mediated system capable of functioning as an organometallic molecular brake.[10] However, very little is known about the interaction of *unsubstituted* rigid molecular fragments although even relatively small hydrogen atoms can cause severe steric repulsion due to spatial proximity and orientation.

In this paper we continue the study of polycyclic molecules incorporating multi-bladed fragments such as triptycene or barrelene, and flat aromatic groups, e.g. indenyl or phenyl. The internal rotational barrier about the single carbon–carbon linkage between these fragments was evaluated by variable-temperature NMR spectroscopy, or by monitoring the kinetics of isomerisation. The key finding is that the rate of intramolecular rotation is sensitive to very fine distinctions in the geometries and orientation of the interconnected moieties.

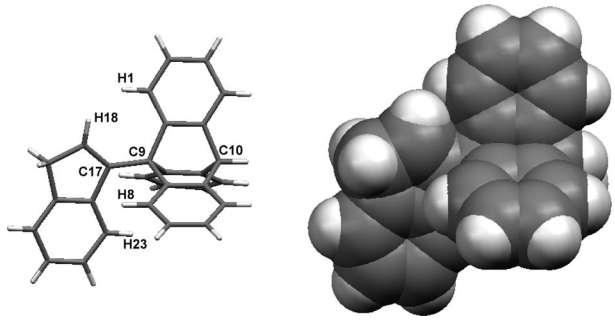

Figure 1. In 9-(3-indenyl)triptycene (**1a**) rotation of the indenyl moiety has to overcome a steric barrier of about 12 kcal mol^{-1} arising from repulsion between H(23) of the indene with the triptycene hydrogens H(1), H(8) and H(13).

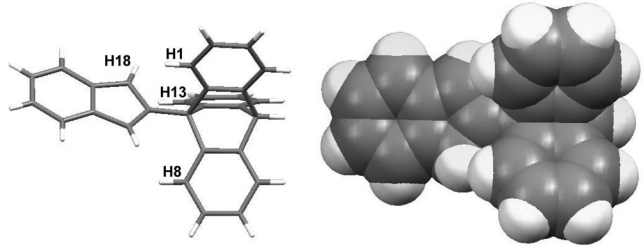

Figure 2. In 9-(2-indenyl)triptycene (**1b**) the H(1), H(8) and H(13) need not approach closer than 1.5 Å to H(18), leading to a significantly lower rotational barrier.[8b]

Results and Discussion

It has previously been shown that in 9-(3-indenyl)triptycene (**1a**) the proximity of the six-membered ring of the indenyl fragment to the triptycyl paddlewheel engenders a 12 kcal mol^{-1} rotation barrier;[8a] this contrasts with the low barrier to rotation observed in 9-(2-indenyl)triptycene (**1b**).[8b] This drastic difference can be readily rationalised by examining the X-ray crystal structures of both isomers, shown also in space-filling style in Figures 1 and 2, respectively.

The intramolecular H···H repulsion interactions can be treated in a manner similar to the approach first applied to 2,2′-substituted biphenyls.[9] In their systematic study Bott, Field, and Sternhell showed that the severity of steric interactions can be approximated by "apparent overlap", *r**, which is defined as the projection of the van der Waals radii in *a hypothetical structure where there is no distortion of bond angles and lengths*.[9b,11] In our study, the experimentally determined molecular structure of **1a** underwent a simple computer modelling procedure involving an analogous "virtual rotation" of the indenyl fragment about the indenyltriptycyl single bond in the 3-indenyl isomer **1a** with no other geometric changes. This indicated that the nominal *Closest Approach Distance* (*CAD*) for H(1)···H(23) is a mere 0.3 Å, while in the 2-indenyl isomer **1b** the analogous H(1)···H(18) CAD is 1.5 Å. Of course, it is reasonable to assume that a clash of these two hydrogens in **1a** can be partially alleviated by bending the indenyl moiety away at the opportune moment. Indeed, even in the observed X-ray crystal structure of **1a**, whereby the indenyl is positioned between two blades, and which presumably represents a potential energy minimum, the indenyl moiety is bent away from the threefold axis of the triptycyl such that the angle C(10)–C(9)–C(17) is 172°.

While the rotational barriers in the 9-indenyltriptycenes **1a** and **1b** apparently are determined by repulsion between hydrogen atoms in the indenyl fragments and *one* of the blades of the triptycene, it is noteworthy that in the isomeric methano-bridged phenanthrenyl-anthracene **1c** (Figure 3) the rotational barrier exceeds 18 kcal mol^{-1}.[8b] In this latter

case, an analysis of its structure indicates the *simultaneous* approach of *two pairs* of hydrogen atoms with CAD values of 0.3 and 1.2 Å leading to an estimated total steric overlap of 3.3 Å. As noted by Sternhell,[9b] the severity of a non-bonded interaction is not determined solely by the size of the interacting fragments, but also by the geometry of the system and its mode of relaxation, in particular its resistance to bond bending or stretching.[11] Moreover, it was suggested that one could predict rotational barriers by using the additivity of pairwise steric contributions,[9b] but this approach has since been questioned.[9d]

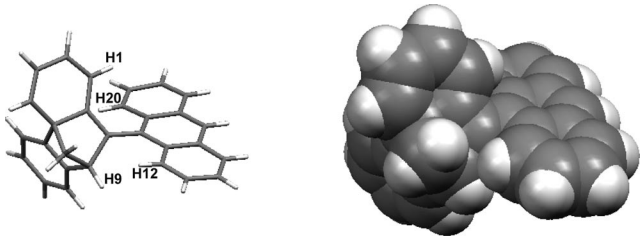

Figure 3. Rotation of the anthracene moiety in the methano-bridged phenanthrenyl derivative **1c** has to overcome two simultaneous repulsion interactions, H(1)–H(20) and H(9)–H(12), such that the barrier exceeds 18 kcal mol^{-1}.

Parallels may be drawn with 2,2′,6,6′-tetrasubstituted biphenyls in which rotation about the single bond linking the aryl rings would engender two simultaneous steric interactions; such systems yield configurationally stable atropisomers. In contrast, analogous rotations in 2,2′-disubstituted biphenyls may proceed via a *transoid* transition state, whereby the bulky substituents can avoid each other.[4a,4e]

Accordingly, we chose to design, synthesise and study a range of molecules in which two or more rigid polycyclic systems were linked by a carbon–carbon single bond. Herein we show that the rotational barrier can significantly change depending on very subtle differences in the orientation and position of hydrogen atoms or other functional groups attached to the core cyclic systems.

Indenylanthracenes

Table 1 summarises the available data on the rotational barriers and nominal closest approach distances, CADs, and *r** values in new and previously published molecules of three types: indenylanthracenes, biindenyls and three-bladed systems (triptycenes and barrelenes).

Having established that the rotational barriers in the 9-indenyltriptycenes **1a** and **1b** depend on the site of attachment to the indenyl fragment, we wished to compare the situation with that of their synthetic precursors 9-(3-indenyl)anthracene (**2a**) and 9-(2-indenyl)anthracene (**2b**) (Scheme 2). In **2a** and **2b** an sp^2–sp^2 carbon–carbon single bond links two planar aromatic fused systems in such a fashion that the dihedral angles between the anthracenyl and indenyl planes are 74° and 70°, respectively. Such a conformation was to be expected because coplanarity of the indenyl and anthracenyl fragments is disfavoured both sterically and electronically.[8b]

Table 1. Internal rotation barriers, $\Delta G^{\neq}$, nominal Closest Approach Distances, CADs, and *r** values in the polycyclic systems **1**–**20**.

	$\Delta G^{\neq}$ [kcal mol^{-1}]	H of first fragment	H of second fragment	CAD [Å]	Overlap,[b] *r**	Ref.
1a	12 ± 0.5	1	23	0.3	2.1	[8a]
1b	<8	1	18	1.5	0.9	*c*
1c	>18[a]	1	20	0.3	3.3	[8b]
		9	12	1.2		
3a	25 ± 0.5[a]	1	17	0.3	3.3	[c]
		8	12	1.2		
3b	13.5 ± 0.5[a]	1	12	1.15	2.4	[c]
		8	17	1.25		
rac-**9**	14.5 ± 0.5[a]	8	7′	0.9	3	[c]
		7	8′	0.9		
meso-**9**	14.8 ± 0.5[a]	7	16	0.9	3.1	[c]
		8	15	0.8		
10	<9	1	18	0.7	1.7	[c]
13	<9	1	14	1.05	1.35	[c]
14	<9	1	14	1.0	1.4	[c]
15	15.3 ± 0.5[a]	14	1	0.7	3	[c]
		18	O	1.65		
16	<9	1	14	0.85	1.55	[c]
19	<9	4	12	1.6	0.8	[c]
20	>23[a]	1	14	0.9	2.95	[c]
		8	18	0.95		

[a] Two close H···H contacts are attained simultaneously. [b] *r** = Σ(van der Waals radii) – Σ(CAD).[9b] [c] This work.

The ^{1}H and ^{13}C NMR spectra of **2a** and **2b** reveal that the external rings of the anthracenyl fragment are equivalent, even at low temperature; this is explicable by invoking a simple oscillation process that generates time-averaged C_s symmetry whereby the indenyl ring plane is orthogonal to the anthracene plane. Moreover, even if the indenyl were to rotate through the anthracenyl plane, thus engendering effective C_{2v} symmetry, such a process would still be undetectable since the outer anthracene rings are already equivalent. To probe the barriers in such systems, it is necessary to prepare the 9,10-diindenyl analogues **3a** and **3b**, assuming their rotational barriers to be identical (or at least very similar) to the undetectable processes in **2a** and **2b**, respectively. The crucial point is that a 180° rotation of either of the indenyl rings in **3a** leads to interconversion of the chemically distinguishable atropisomers *syn*-**3a** (effectively C_{2v}) and *anti*-**3a** (effectively C_{2h}) – a process that can be monitored by NMR spectroscopy.

9,10-Bis(2-indenyl)anthracene (**3b**) was prepared by the palladium-catalysed coupling of 9,10-dibromoanthracene (**4**) with 2-indenylboronic acid (**5**) (Scheme 3) analogously to the previously described synthesis of **2b**.[8b,12] In contrast, the preparation of the 3-isomer **3a** via a palladium-catalysed Heck reaction was unsuccessful. Under these conditions, the formation of polycyclic indeno-dihydroanthrylenes was predominant, as had been observed in other Pd-catalysed reactions involving anthracenes.[8b,13] However, 9,10-bis(3-indenyl)anthracene (**3a**) was successfully prepared by the Stille coupling of 9,10-dibromoanthracene (**4**) with 1-(trimethylstannyl)indene (**6**). The mono-coupled product, 9-bromo-10-(3-indenyl)anthracene (**7**), was also isolated after chromatographic separation; its

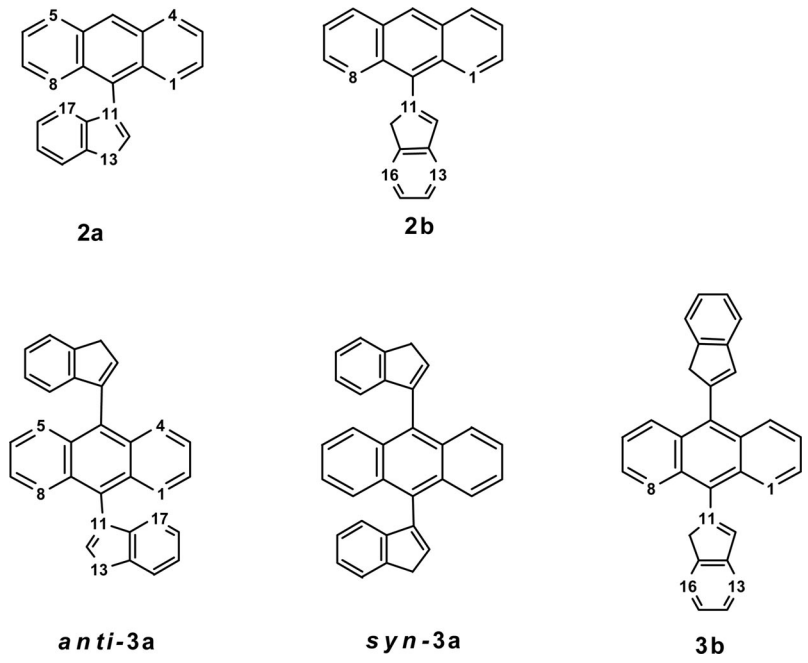

Scheme 2. 9-Indenylanthracenes **2** and 9,10-di-indenylanthracenes **3**.

X-ray crystal structure is shown in Figure 4, and the dihedral angle between the indenyl and bromoanthracenyl planes is 65°.

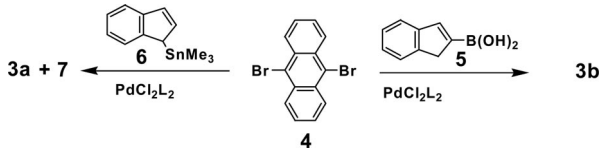

Scheme 3. Synthesis of the di-indenylanthracenes **3a** and **3b**.

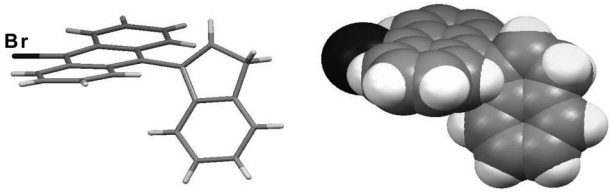

Figure 4. X-ray crystal structure and spacefill view of 9-bromo-10-(3-indenyl)anthracene (**7**).

It transpired that, as indicated by NMR, 9,10-bis(3-indenyl)anthracene, **3a**, is a nearly equimolar mixture of *syn*- and *anti*-atropisomers that can be separated by column chromatography. However, the assignment of either one as *syn* or *anti* cannot be unambiguously determined spectroscopically. Fortunately, one atropisomer of **3a** yields X-ray quality crystals, and the structure of *anti*-**3a** appears in Figure 5; in addition, the structure of the bis(2-indenyl) isomer **3b** is shown in Figure 6. The indenyl rings adopt dihedral angles of 81.5° (*anti*-**3a**) and 81.7° (**3b**) with the anthracene plane. A computer-assisted virtual rotation of the indenyl fragment about the single bond (whilst maintaining the remaining geometry) shows that the CAD for H(1)···H(17) in *anti*-**3a** is 0.3 Å, suggesting the existence of a very high rotational barrier, even allowing for the geometric perturbations that must certainly occur. In contrast, the analogous CAD in **3b**, H(1)···H(12), exceeds 1.1 Å. Moreover, in **3b** the *syn*- and *anti*-rotamers are disordered in the solid state such that the methylene and methine sites in the five-membered rings are each 50% occupied.

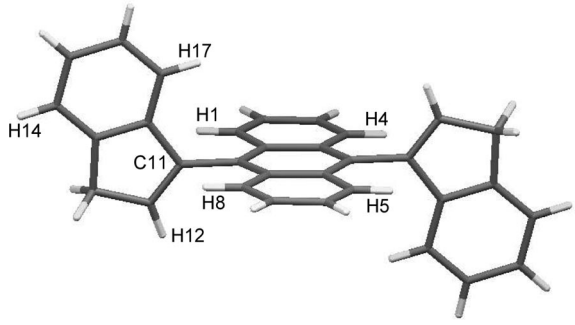

Figure 5. X-ray crystal structure of 9,10-di-(3-indenyl)anthracene (*anti*-**3a**). Rotation of the indenyl fragments is severely hindered because of simultaneous close contacts in the pairs H(8)–H(12) (CAD = 0.3 Å) and H(1)–H(17) (CAD = 1.2 Å).

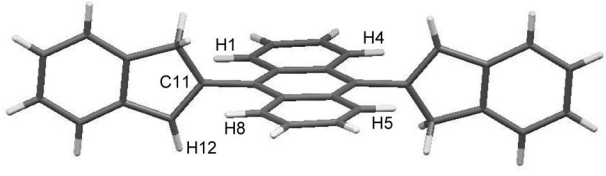

Figure 6. X-ray crystal structure of 9,10-di-(2-indenyl)anthracene (**3b**). Rotation is markedly less hindered since the nominal closest approach distance between H(1) and H(12) is 1.15 Å.

Although the ^{1}H NMR spectra of the two atropisomers of 9,10-bis(3-indenyl)anthracene, **3a**, are very similar, it is possible to identify key differences in the 6.5–7.0 ppm region, and hence to follow the interconversion of *anti*-**3a** and *syn*-**3a** at different temperatures. The barrier was evaluated as ca. 25 kcal mol^{-1}, approximately twice the value found in the corresponding three-bladed system 9-(3-indenyl)triptycene (**1a**). As noted above and depicted in Figure 1, the triptycene **1a** adopts a structure such that, although the six-membered ring of the 3-indenyl moiety is positioned between two blades, the five-membered ring is seen to twist out of the molecular mirror plane so as to minimise the interaction between H(1) and H(18). This distortion presumably raises the energy of the ground state and so slightly lowers the apparent barrier. Moreover, simulation of virtual rotation in **1a** reveals that as the benzo ring of the 3-indenyl passes a triptycyl blade, the five-membered ring can bend into the space between the other two blades, thus minimising the energy cost of the rotation. This "duck-and-dodge" mechanism cannot be realised in the case of the bis(3-indenyl)anthracenes **3a**, *in which two unfavourable coplanar H···H contacts are attained simultaneously.* Moreover, the observed rotational barrier of 25 kcal mol^{-1} is without a doubt significantly higher than that estimated on the basis of empirical correlation given by Sternhell.[9b]

Although the variable-temperature 500 MHz ^{1}H NMR spectra of 9,10-bis(2-indenyl)anthracene (**3b**) did not reveal the presence of *syn* and *anti* atropisomers, this phenomenon was observable in the ^{13}C regime. Furthermore, coalescence of each of the two pairs C(9) *syn*/*anti* and C(11) *syn*/*anti* resonances at –26 °C indicated a barrier of ca. 13.5 kcal mol^{-1}, in good agreement with estimated nominal CAD in this molecule.

1,1′-Biindenyls

We recently reported that the isomeric *meso*- and *racemic*-2,2′-disubstituted-1,1′-biindenyls can readily be prepared by oxidative dimerisation of lithiated indenes.[14] Furthermore, it was shown that rotation about the central carbon–carbon bond in *meso*-2,2′-diphenyl-1,1′-biindenyl (**8**) is slow as evidenced by its NMR spectrum in conjunction with DFT-level calculations.[14] Consequently, it was of interest to probe the rotational barriers about the central carbon–carbon bond in the related methyl-substituted 1,1′-biindenyls **9** and to correlate these activation energies with their molecular structures.

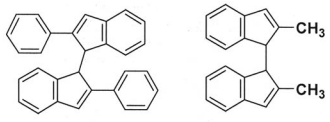

8 9

The 2,2′-dimethyl-1,1′-biindenyls **9** were prepared by treatment of 1-lithio-2-methylindene with $CuCl_2$ and, after chromatographic separation, the *racemic* and *meso* isomers were characterised by X-ray crystallography. As shown in Figure 7, both molecules adopt a *gauche* conformation: in *rac*-**9** the dihedral angle H(1)–C(1)–C(1′)–H(1′) is 58°, and the corresponding angle, H(1)–C(1)–C(9)–H(9), in *meso*-**9** is 66°. It is noteworthy that in the conformation adopted by *rac*-**9** in solid state the H(1) and H(1′) hydrogens are positioned *between* two widely-separated methyl substituents, as shown in Scheme 4 for *rac*-**9b**.

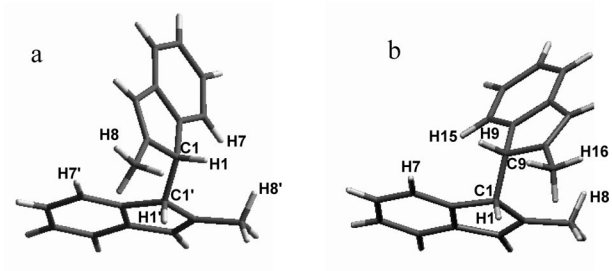

Figure 7. X-ray crystal structures of (a) *rac*-**9** and (b) *meso*-**9**. In these dimers, rotation about the central C(1)–C(1′) or C(1)–C(9) bond is slowed (barrier about 15 kcal mol^{-1}) by simultaneous close approach of H(7)–H(7′) and the hydrogens of the methyl groups at C(8) and C(8′), in *rac*-**9**, and of H(7)–H(15) and the methyl hydrogens, such as H(8)–H(16), in *meso*-**9**.

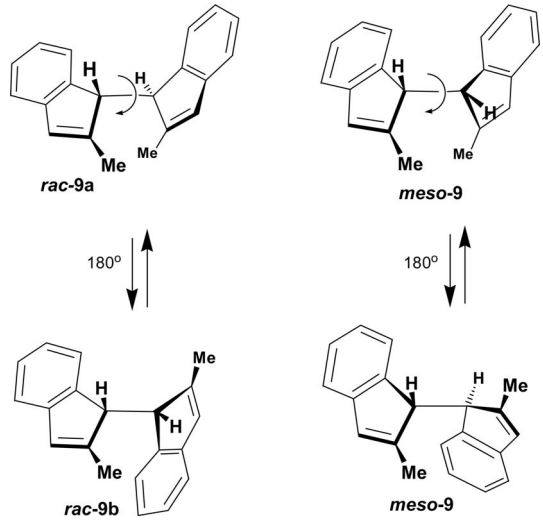

Scheme 4. A 180° rotation about the central bond in *rac*-**9a** leads to a different C_2 isomer, *rac*-**9b**. In contrast, the analogous rotation in *meso*-**9** merely interconverts enantiomers.

Interestingly, the room temperature ^{1}H NMR spectra of both *rac*-**9** and *meso*-**9** were broad and unresolved in both the aromatic and aliphatic regions. However, lowering the temperature to –15 °C led to full decoalescence of all signals (Figure 8). At that temperature the racemic isomer of **9** is represented by a 42:58 mixture of two slowly interconverting C_2-symmetric rotamers, *rac*-**9a** and *rac*-**9b** (Scheme 4), of which the latter is presumably the more stable since it is the only one found in the solid state. As the temperature is ramped up, the NMR signals broaden and eventually coalesce at ca. 35 °C; the rotational barrier is approximately 14.5 kcal mol^{-1} (Table 1). While this barrier is perhaps higher than would have been expected on the basis of relatively long (0.9 Å) crystallographically-determined CAD in this molecule, one should note that the

interconversion of *rac*-**9a** and *rac*-**9b** requires simultaneous close approach of both the methyls and the indenyls of the molecule.

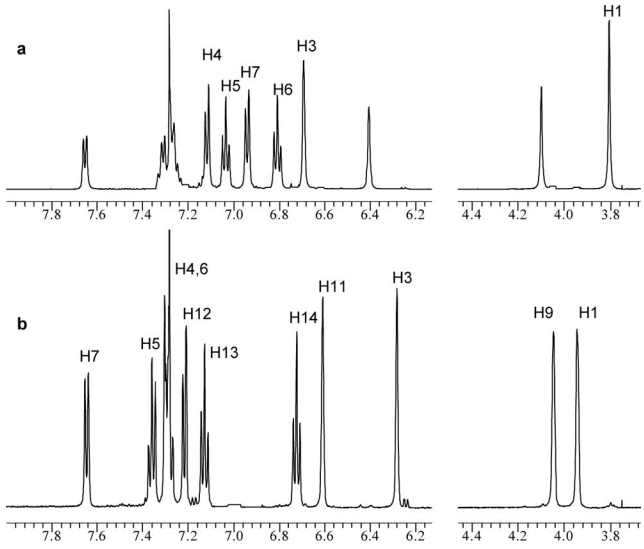

Figure 8. 500 MHz ^{1}H NMR spectra (–15 °C, $CDCl_3$) of (a) *rac*-**9** as an equilibrium mixture of conformers *rac*-**9a** (42%) and *rac*-**9b** (58%, assignments shown); (b) note that in *meso*-**9** the H_1 and H_9 protons are anisochronous.

Unlike dimeric *rac*-**9** that retains its C_2 symmetry whatever the rotamer conformation, *meso*-**9** loses all symmetry elements unless the central H–C–C–H dihedral angle is 0° or 180°, giving rise to either a single mirror plane (C_s) or an inversion centre (*Ci*), respectively. At low temperature (–15 °C), *meso*-**9** is represented by an individual conformer whose NMR spectrum indicates the presence of two non-equivalent 2-methylindenyl moieties, in accord with its unsymmetrical structure in solid state (Figure 7, b). Rotation about the central C(1)–C(9) bond leads to enantiomerisation (see Scheme 4) in which the two methylindenyl moieties exchange roles. Coalescence of the H(1) and H(9) resonances at 30 °C indicates a rotational barrier of ca. 15 kcal mol^{-1}, presumably via a mirror-symmetric transition state. This finding is in good agreement with our earlier data on 2,2′-diphenyl-1,1′-biindenyl (*meso*-**8**), whereby the substituents at the 2-indenyl positions become closely proximate as the enantiomerisation proceeds. We note, however, that DFT calculations on the diphenyl system **8** revealed that the central carbon–carbon bond lengthens markedly in the transition state.[14]

Substituted Triptycenes

It has long been known that the rotation barriers in 9-substituted triptycenes are very responsive to the steric size and orientation of the substituent;[3] for instance, the barrier reaches 16 kcal mol^{-1} in 9-(chloromethyl)triptycene.[15] As discussed above, the barrier to paddlewheel rotation in indenyltriptycenes **1** is also very sensitive to the mode of attachment of the indenyl moiety (Scheme 1). Accordingly, one might anticipate that variations in the structure of the paddlewheel will also challenge the rotational barrier. We

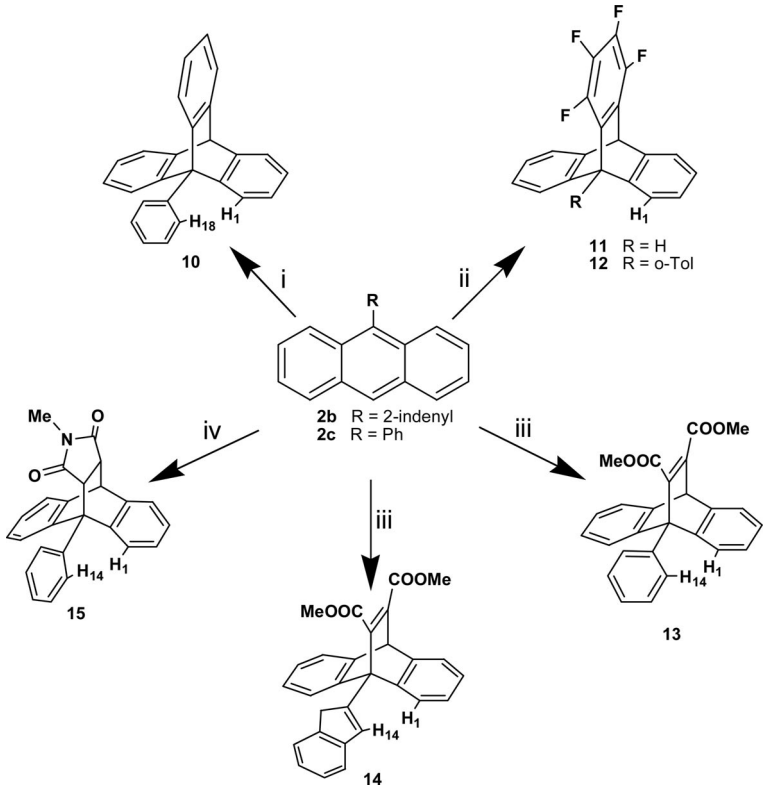

Scheme 5. Preparation of three-bladed molecules **10**–**15** from substituted anthracenes **2b** or **2c**. Reagents: (i) benzyne; (ii) tetrafluorobenzyne; (iii) DMAD; (iv) *N*-methylmaleimide.

here describe the syntheses, X-ray crystal structures and dynamic NMR behaviour of several closely related molecules, **10**–**20**, (Schemes 5 and 6) in each of which a three-bladed paddlewheel is linked to either a phenyl or an indenyl moiety.

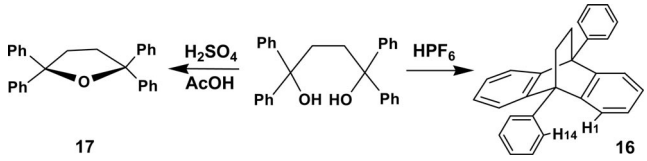

Scheme 6. Syntheses of the diphenyl-dibenzodihydrobarrelene derivative **16** and tetraphenyltetrahydrofuran (**17**).

Earlier reports on rotational barriers in 9-aryltriptycenes appear to suggest that rotation is fast on the NMR time-scale in these symmetrical molecules attributable, possibly, to steric hindrance raising the energy of the ground state.[3] The parent compound, 9-phenyltriptycene (**10**), was therefore prepared and characterised by X-ray crystallography and variable-temperature NMR spectroscopy. The structure appears as Figure 9, and reveals that the phenyl moiety is bent off the threefold axis of the triptycene by 6° indicating a slightly unbalanced steric repulsion. Nevertheless, as with 2-indenyltriptycene (**1a**), there is no evidence of slowed rotation of the phenyl fragment on the NMR time-scale at temperatures down to –60 °C, indicating a rotational barrier well below 10 kcal mol^{-1}. This is in a good agreement with the calculated CAD of 0.7 Å between H(18)/H(22) of the phenyl fragment and H(1)/H(8)/H(13) of the blades.

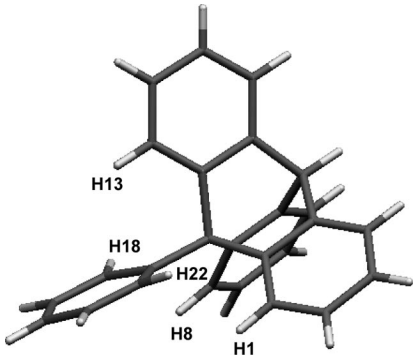

Figure 9. Molecular structure of 9-phenyltriptycene (**10**) showing a possible close contact between H(18)/H(22) and *one* of H(1)/H(8)/H(13) of the triptycene.

Another way to break the threefold symmetry of a triptycene involves the functionalisation of one, or more, of the blades. Although the Diels–Alder addition of tetrafluorobenzyne to anthracene to form 1,2,3,4-tetrafluorotriptycene (**11**) was first reported in 1968,[16] we are unaware of any structural characterisation of the parent compound, nor of any 9-substituted derivatives. The X-ray crystal structure of 1,2,3,4-tetrafluorotriptycene is shown in Figure 10, and the geometry deviates only slightly from ideality: the interplanar angle between the two benzo rings (123.1°) is somewhat larger that those between the tetrafluorobenzo ring and its neighbours (120.5° and 116.4°). Moreover, there are two independent molecules of **11** in the unit cell, one of which exhibits a disorder between the tetrafluorobenzo ring and one of its C_6H_4 partners.

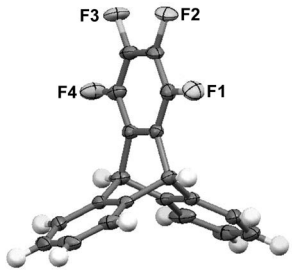

Figure 10. Molecular structure of 1,2,3,4-tetrafluorotriptycene (**11**); thermal ellipsoids at 50%.

Interestingly, we note that the variable-temperature NMR behaviour of the substituted 9-(*o*-tolyl)-1,2,3,4-tetrafluorotriptycene derivative **12** has been interpreted in terms of an oscillation process whereby the largest barrier would require the methyl to rotate past the fluorinated benzo ring.[3a]

Substituted Barrelenes

Having established that paddlewheel rotation in both 9-(2-indenyl)triptycene (**1b**) and 9-phenyltriptycene (**10**) is rapid at ambient temperature, we chose to study the analogous 11,12-bis(methoxycarbonyl)dibenzobarrelene derivatives **13** and **14** to probe the effect of incorporating the more sterically demanding ester substituents. These molecules were prepared by the Diels–Alder cycloaddition of DMAD to the corresponding substituted anthracenes, as shown in Scheme 5.

The X-ray structures (Figure 11) reveal that in these molecules the dibenzobarrelene core almost retains its pseudo-threefold symmetry. In the phenyl derivative, **13**, the interplanar angles between the two peripheral benzo rings and those between the benzo rings and the C(11)–C(12) double bond are 121.8°, 123.2° and 115.0°, respectively: in the 2-indenyl system **14** the corresponding angles are 121.2°, 120.3° and 118.5°. Moreover, the phenyl substituent in **13**, and the 2-indenyl fragment in **14**, deviate slightly from coplanarity with the C(11)–C(12) double bond bearing the methoxycarbonyl groups. In **13**, the dihedral angle C(12)–C(9)–C(13)–C(18) is 20°, and the angular distortion of the phenyl from C(10)–C(9) axis of the paddlewheel is 4.4°; in **14**, the dihedral angle C(12)–C(9)–C(13)–C(19) is 10°, and the angular distortion of the indenyl from C(10)–C(9) axis of the paddlewheel is only 3.5 degrees. To allow access to this conformation the adjacent methoxycarbonyl groups sacrifice their conjugative interaction with the double bond by rotating through ca. 75° away from the substituent at C(9). Interestingly, in the parent compound, dimethyl dibenzobarrelene-11,12-dicarboxylate, the torsion angles C(11)=C(12)–C=O and C(12)=C(11)–C=O are 116° and 164°, again revealing a marked twisting of the ester moieties away from the double bond.[17]

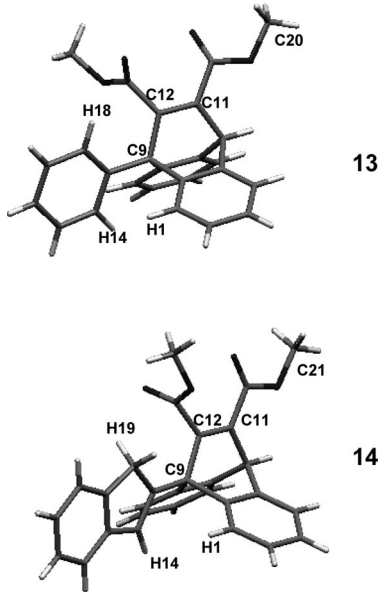

Figure 11. Molecular structures of dimethyl 9-phenyldibenzobarrelene-11,12-dicarboxylate, **13**, and dimethyl 9-(2-indenyl)dibenzobarrelene-11,12-dicarboxylate, **14**.

The simplicity of the NMR spectra of both **13** and **14** indicates that rapid rotation occurs even at –70 °C, signifying in each case a low barrier about the C(9)–(C13) linkage. It has previously been shown that an out-of-plane carbonyl group poses no significant barrier to rotation in 2-substituted biphenyls.[9c] Similarly, in the case of **13** or **14**, since the esters are twisted out of the plane of the double bond they do not significantly hinder rotation of the 9-indenyl or 9-phenyl groups. These low barriers are consistent with CADs in excess of 1 Å (Table 1) in the absence of double steric interactions – behaviour similar to that seen in the previously discussed triptycenes **1a**, **1b** and **10**.

Substituted Dihydrobarrelenes

Further studies have been carried out using 9,10-diphenyl-11,12-dihydrodibenzobarrelene (9,10-diphenyl-9,10-ethanoanthracene) (**16**) and also the Diels–Alder adduct **15** prepared by addition of *N*-methylmaleimide to 9-phenylanthracene. Molecule **16** was prepared by an elegant intramolecular double cyclisation[18] of 1,1,4,4-tetraphenylbutane-1,4-diol in hexafluorophosphoric acid medium (Scheme 6). Interestingly, cyclisation using H_2SO_4 in acetic acid yields pure 2,2,5,5-tetraphenyltetrahydrofuran (**17**)[19] in which the bulky phenyl substituents engender a C_2-symmetric structure (Figure 12) such that pairs of phenyls adopt dihedral angles of 77° ± 1° and 47° ± 1° relative to the plane containing the oxygen and its adjacent carbons.

The NMR spectrum of the diphenyl-ethanoanthracene **16** at room temperature revealed that the *ortho* and also the *meta* positions of both phenyls were equivalent, as were the blades of dibenzobicyclooctane moiety. Variable-temperature measurements confirmed that no significant slowed rotation was evident at –60 °C. This finding is consistent with

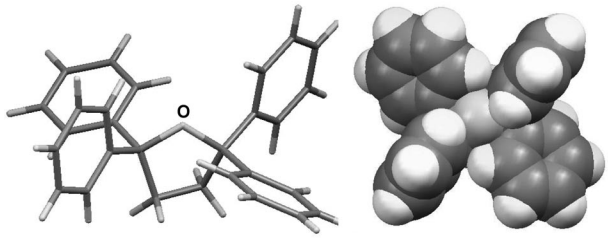

Figure 12. X-ray crystal structure of 2,2,5,5-tetraphenyltetrahydrofuran (**17**): bird's eye view and edge-on view (space-filling) emphasising the C_2 character of the molecule.

only rather slight steric strain associated with the phenyldibenzocyclooctane interaction, as is apparent from the X-ray crystal structure of **16** (Figure 13). There is a substantial CAD of 0.85 Å between H(1)/H(8) and H(14)/H(18), and no double steric repulsion is involved.

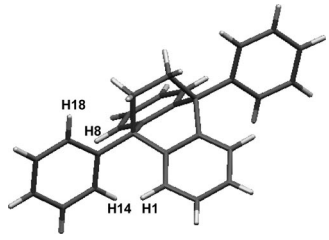

Figure 13. X-Ray crystal structure of 9,10-diphenyl-11,12-dihydrodibenzobarrelene (**16**). In this molecule, phenyl rotation is fast on the NMR time-scale, since the H(1)/H(14) CAD is relatively long, and no double interactions are involved.

We note that as the interplanar angle between peripheral benzo rings gradually approaches planarity, the configuration of the transition state on the rotation energy profile would resemble that of a substituted anthracene, i.e. double steric repulsions would be engendered. In the triptycenes and barrelenes discussed above, the interplanar angle between peripheral benzo rings is approximately 120°. However, in the dihydrobarrelene, **16**, the anthracene framework is somewhat closer to planarity such that this value is now 134°, while the angle between the benzo rings and the ethano-bridge is 113° ± 2°. The corresponding angles in the *N*-methylmaleimide–9-phenylanthracene Diels–Alder adduct **15** are 131.2° and 114.4°, respectively.

In the *N*-methylmaleimide/9-phenylanthracene Diels–Alder adduct **15** (Figure 14) the incorporation of the pyrrolidone fragment renders the two aromatic blades non-equivalent, and so slowed rotation of the phenyl substituent would split the degeneracy of its *ortho* and *meta* positions. In the room temperature 500 MHz ^{1}H NMR spectrum of **15** the signals assignable to the peripheral benzo rings are clearly resolved whereas the *ortho* and *meta* positions of the phenyl ring are broadened. However, at –15 °C the *ortho* protons (at δ = 8.10 and 7.41) and *meta* protons (at δ = 7.67 and 7.53) have clearly decoalesced (Figure 15), indicating that rotation has slowed on the NMR timescale. Subsequent observation of coalescence for the *ortho* and *meta* resonances at 70 °C and 40 °C, respectively, yielded a substantial rotational barrier of 15.5 ± 0.5 kcal mol^{-1} for this

process. It is unlikely that this barrier is associated with the H(1)···H(14) CAD of 0.7 Å. However, a bending of the phenyl through 7.6° away from C(9)–C(10) axis of the bicyclooctane core implies a steric repulsion between the carbonyl oxygen, O(1), and the phenyl *ortho* hydrogens H(14)/H(18) for which the CAD is 1.65 Å. Bearing in mind the substantially larger atomic radius of the carbonyl oxygen compared to hydrogen, it is more likely that this is the interaction that increases the rotational barrier. Interestingly, NMR spectroscopic data on **15** at elevated temperatures suggest that the Diels–Alder addition of *N*-methylmaleimide to 9-phenylanthracene is reversible; this parallels the very recent report by Lehn that reversible Diels–Alder reactions of cyanoethylenes with 9,10-dimethylanthracene can be used in fluorescent optical switches.[20]

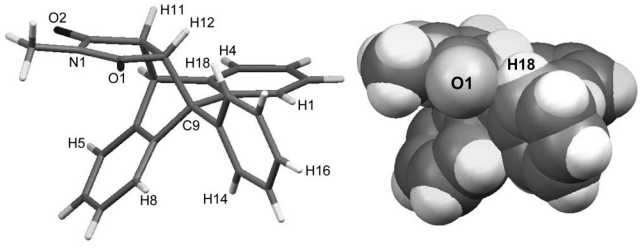

Figure 14. The X-ray crystal structure of 11,12-(*N*-methylpyrrolidino)-9-phenyldibenzobarrelene (**15**) suggests that close approach of H(18) and carbonyl O(1) creates the observed substantial phenyl rotation barrier of 15.5 kcal/mol.

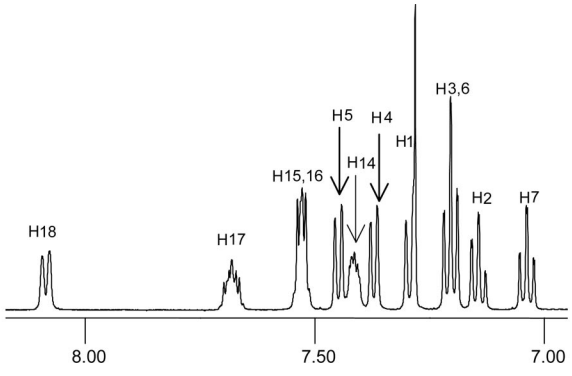

Figure 15. 500-MHz ^{1}H NMR spectrum of the Diels-Alder adduct **15** in the aromatic region.

1,6-Diphenyl-7,8,9,10-dibenzo-2,5-dioxabicyclo[4.2.2]decane

In light of the already discussed correlation between the rotational barriers in paddlewheel-type systems and the room for manoeuvre available to substituents at C(9), it was decided to attempt to construct a molecular system in which movement of the phenyl substituents was constrained by modifying the length of the bridge between C(9) and C(10). To this end, treatment of anthraquinone with phenylmagnesium bromide furnished 9,10-diphenyldihydroanthracene-9,10-diol **18** (Scheme 7, Figure 16). The structure (Figure 16, a) confirms that the previously postulated[21] *trans* configuration of the two hydroxy groups was correct. The diol **18** was readily converted into its dimethyl ether **19** (Figure 16, b). The variable-temperature ^{1}H NMR spectra of **19** indicate that the phenyl groups are apparently free to rotate at –60 °C despite the fact that this rotation would involve simultaneous approach of the H(4)/H(12) and H(5)/H(16) pairs. The virtual rotation analysis revealed that no significant H···H repulsive interactions are present in this molecule since the CAD is very large (1.6 Å).

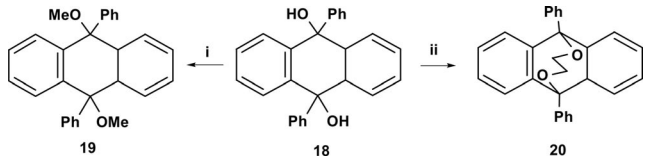

Scheme 7. Reagents and conditions: (i) methanol, H_2SO_4, reflux, 3 h, 100%; (ii) ethylene glycol, toluene, TSA, 60 °C, 24 h, 52%.

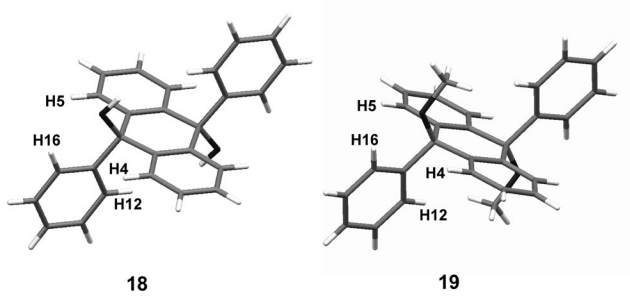

Figure 16. X-Ray crystal structures (a) of the *trans*-diol **18**, and (b) the dimethyl diether **19**.

When the *trans*-diol **18** was heated with ethylene glycol in toluene in the presence of acid, the novel bicyclic ether **20** was isolated in 52% yield, and its structure appears as Figure 17. Since the initial configuration of the diol **18** is *trans*, and both ether linkages in **20** are necessarily on the same side of the original anthracene plane, the reaction evidently proceeds with inversion of configuration at one of the benzylic centres. The peripheral benzo rings in **20** are no longer coplanar as in the diol **18**, but the dihedral angle is 166°, substantially larger than the value of 134° observed in the 9,10-ethanoanthracene **16**. Clearly, extension of the bridge from a two-atom chain in **16** to a four-atom chain in **20** flattens the central ring system, pushes the phenyls at the bridgehead positions into the narrow space between the *ortho* hydrogen atoms of the peripheral rings and severely limits their freedom.

Virtual rotation simulation for **20** shows that the shortest H···H distances between the phenyl *ortho*-hydrogen atoms, H(14)/H(18), and the paddlewheel blade hydrogen atoms H(1)/H(8) are attained simultaneously with a CAD of ca. 0.9 Å. Unlike the situation in triptycenes **1** and **10**, or the three-bladed barrelene derivatives, **10**, **11**, **13**–**16**, the phenyl moiety cannot escape strong lateral repulsion by bending away and slipping between the blades. Consequently, the phenyls are locked in an orientation perpendicular to the surface of the dihydroanthracene moiety.

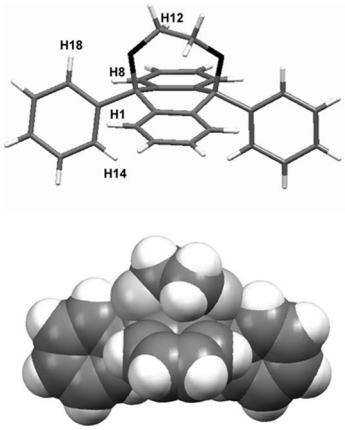

Figure 17. As shown in the X-ray crystal structure of **20**, rotation of the phenyls has to overcome simultaneous repulsion of H(1)/H14 and H(8)/H(18) with CAD 0.9 Å; the space-filling representation of **20** shows the phenyls constrained by the "calipers" of the dibenzobicyclodioxadecane core.

The 500 MHz ^{1}H NMR spectrum of **20** in the aromatic region is shown in Figure 18, and clearly illustrates that all five aromatic protons of the phenyl ring are non-equivalent. The chemical shift separation of about 1.4 ppm reveals very different magnetic environments for the phenyl protons, H(14) and H(18), presumably attributable to the combined effects of the two closely located aromatic ring systems of the paddlewheel. An NMR study over the temperature range 30–90 °C showed no peak broadening nor 2D EXSY exchange between H(14) and H(18); hence, one can only calculate a minimum rotational barrier on the basis of the NMR chemical shift difference between two non-coalescing signals, such as H(15) and H(17), that would be equilibrated if rotation were to occur. These data yield a minimum value for the rotational barrier of 23 kcal mol^{-1}, but it is undoubtedly substantially higher.

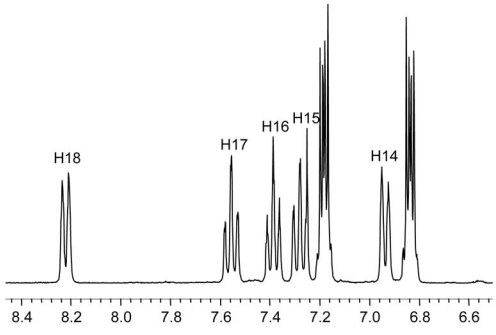

Figure 18. 500 MHz ^{1}H NMR spectrum of the cyclic ether **20** in the aromatic region.

Conclusions

In this paper the factors determining the ease of thermal rotation about a carbon–carbon single bond interconnecting two rigid molecular fragments have been studied. As emphasised by Hunter,[22] solvent effects can also be important parameters, and so in this work all barriers were measured in similar systems (CD_2Cl_2, $CDCl_3$ or $C_2D_2Cl_4$, depending on the temperature required for peak coalescence). The structural parameters of the molecules have been fully established by X-ray crystallography augmented by a computational "virtual rotation" process, and the rotational barriers have been estimated from variable-temperature NMR and kinetic data. The goal was to probe the combination of geometric molecular parameters that led to the sometimes surprisingly high, or low, rotational barriers in polycyclic systems.

Comparison of the rotational barriers for the 3-indenylanthracenes **2a** and **3a** with that for the apparently closely related 3-indenyltriptycene (**1a**) revealed that they can be very different despite the similarity in their nominal H···H Closest Approach Distances (CADs) obtained from the virtual rotation of molecular fragments. The simultaneous development of two strong steric repulsions between two planar aromatic fused systems renders the rotation about the single C–C bond in 3-indenylanthacenes very slow at room temperature. In the paddlewheel-shaped 3-indenyltriptycene this seemingly equally strong repulsion can be alleviated by an energetically more favourable "duck and dodge" motion of the indenyl moiety. The idea that not only the strength of an individual steric interaction, but also the number of simultaneously attained interactions, and the ability of the molecular fragments to adapt to the changing environment and so determine the energy cost of the rotation, helps to rationalise a wide range of new observations in this area.

Thus, the rotational barriers in 2,2′-disubstituted-1,1′-biindenyls are, similarly to 3-indenylanthracenes, governed by strong H···H interactions in the transition state, and can be interpreted in terms of simultaneous steric repulsions and the CADs between hydrogens of the aromatic rings and the substituents. Moreover, one can conclude that the rotational barriers in the 9-aryl-11,12-bis(methoxycarbonyl)dibenzobarrelenes **13** and **14** are no higher than in structurally related 9-substituted triptycenes (8–9 kcal/mol) because in each case the adjacent methoxycarbonyl moiety rotates out of the plane of the dibenzobarrelene blade. So, in the absence of multiple steric repulsion interactions, rotation in these systems is reasonably facile. However, this relatively low rotational barrier can be significantly increased by introducing a rigidly oriented heteroatom pointing in the direction of the rotating phenyl as in the imide **15**.

In this context, the very striking difference (at least 10 kcal mol^{-1}) in the rotational barriers between dihydroanthracene derivatives **19** and **20** can be clearly understood in terms of CADs and multiple steric interactions. In the di-ether **19** a possible double steric repulsion is not realised owing to relatively long CAD; in the bridged di-ether, **20**, the nearly-planar conformation of the benzo blades leads to substantially shorter CADs. Consequently, the rotation of the phenyls is severely restricted because of simultaneous steric interactions with both blades. The combination of steric effects that have been exemplified herein may

have subtle implications for the design of molecular machines, and provide continued motivation for studies in the area of mechano-stereochemistry.[23]

Experimental Section

General: All reactions were carried out under a nitrogen atmosphere unless otherwise stated. Column chromatography separations were carried out on a Buchi Sepacor machine with UV absorbance detector using silica gel particle size 40–63 mm. NMR spectra were acquired on Varian VNMRS 400 and 600 or Inova 500 MHz spectrometers at 25 °C unless otherwise stated. Assignments were based on standard ^{1}H-^{1}H and ^{1}H-^{13}C two-dimensional techniques, and NOE measurements. Rotational barriers were obtained by standard peak coalescence measurements.[24] Melting points were determined on a Gallenkamp instrument in air and are uncorrected. Elemental analyses were carried out by the Microanalytical Laboratory at University College Dublin. Compounds **1a**–**c**,[8] **2a**,[8a] **2b**,[8b] **10**,[25]**11**[16] **16**,[18] **17**,[19] **18** and **19**[21] were prepared as described elsewhere.

9,10-Bis(3-indenyl)anthracenes (3a) and 9-Bromo-10-(3-indenyl)-anthracene (7): To a stirred suspension of the dibromide **4** (0.135 g, 0.4 mmol) in 1,4-dioxane (2 mL), dichloro-bis(tri-*o*-tolylphosphane)palladium (3 mg, 0.004 mmol) and indenyltrimethyltin (0.34 g, 1.2 mmol) were added. The reaction mixture was stirred for 40 h at 120 °C (sealed tube) after which time it was concentrated, extracted with copious amounts of dichloromethane, washed successively with aqueous hydrochloric acid, ammonia, hydrochloric acid, sodium hydrogen carbonate and separated to afford **3a** (102 mg, 63%) as a *syn*/*anti* mixture, and 9-bromo-10-(3-indenyl)-anthracene (**7**) (18 mg, 12%) as a yellow solid. ^{1}H NMR (500 MHz, $CDCl_3$): δ = 8.60 (d, J = 8 Hz, 2 H), 7.90 (d, J = 8 Hz, 2 H), 7.63 (d, J = 7.5 Hz, 1 H), 7.55 (t, J = 7.5 Hz, 2 H), 7.36 (t, J = 7.5 Hz, 2 H), 7.28 (t, J = 7.5 Hz, 1 H), 7.12 (t, J = 7.5 Hz, 1 H), 6.72 (s, 1 H), 6.65 (d, J = 7.5 Hz, 1 H), 3.84 (s, 2 H) ppm. ^{13}C NMR (125 MHz, $CDCl_3$): δ = 146.5, 143.4, 141.8, 135.4, 131.7, 131.0, 130.4, 128.0, 127.1, 126.5, 125.6, 123.0, 120.8, 38.8 ppm. $C_{23}H_{15}Br$ (371.28): calcd. C 74.41, H 4.07, Br 21.52; found C 74.20, H 4.22, Br 21.16. Careful separation of **3a** (2% dichloromethane in cyclohexane) yielded *syn*-**3a** (30 mg) and *anti*-**3a** (60 mg): *anti*-**3a** is a yellow solid; m.p. 295–300 °C (dec.). ^{1}H NMR (500 MHz, $CDCl_3$, numbering as in Scheme 1): δ = 7.96 (d, J = 7 Hz, 4 H, H1, H4, H5, H8), 7.67 (d, J = 7.5 Hz, 2 H, H14, H21), 7.31 (d, J = 7 Hz, 4 H, H2, H3, H6, H7), 7.28 (t, J = 7.3 Hz, 2 H, H15, H22), 7.15 (t, J = 7.3 Hz, 2 H, H16, H23), 6.80 (d, J = 7.5 Hz, 2 H, H17, H24), 6.80 (s, 2 H, H12, H19), 3.87 (s, 4 H, 2× H13, 2× H20) ppm. ^{13}C NMR (125 MHz, $CDCl_3$): δ = 146.8 (C13b), 143.7 (C13a), 142.4 (C9), 135.0 (C12), 131.1 (C11), 130.0 (C4a), 126.9 (C1), 126.4 (C16), 125.1 (C2), 125.0 (C15), 123.8 (C14), 121.2 (C17), 44.5 (C13) ppm. $C_{32}H_{22}$ (406.53): calcd. C 94.55, H 5.45; found C 94.16, H 5.94. *syn*-**3a** is a yellow solid; m.p. 295–300 °C (dec.). ^{1}H NMR (500 MHz, $CDCl_3$): δ = 7.96 (d, J = 7 Hz, 4 H, H1, H4, H5, H8), 7.67 (d, J = 7.5 Hz, 2 H, H14, H21), 7.30 (t, J = 7 Hz, 4 H, H2, H3, H6, H7), 7.28 (t, J = 7.3 Hz, 2 H, H15, H22), 7.17 (t, J = 7.3 Hz, 2 H, H16, H23), 6.85 (d, J = 7.5 Hz, 2 H, H17, H24), 6.75 (s, 2 H, H12, H19), 3.85 (s, 4 H, 2× H13, 2× H20) ppm. ^{13}C NMR (125 MHz, $CDCl_3$): δ = 146.9 (C13b), 143.7 (C13a), 142.4 (C9), 135.1 (C12), 131.2 (C11), 130.0 (C4a), 126.9 (C1), 126.4 (C16), 125.2 (C2), 125.1 (C15), 123.9 (C14), 121.1 (C17), 39.0 (C13) ppm. $C_{32}H_{22}\cdot 0.5C_6H_{12}$ (448.61): calcd. C 93.71, H 6.29; found C 93.80, H 6.07 (from cyclohexane).

9,10-Bis(2-indenyl)anthracene (3b): To a stirred suspension of **4** (0.27 g, 0.8 mmol) in a mixture of ethanol (6 mL) and toluene (12 mL), the boronic acid, **5** (0.32 g, 2 mmol), sodium carbonate (0.42 g, 4 mmol), dichloro-bis(diphenylphosphanylferrocene)palladium (8 mg, 0.01 mmol) were added. The reaction mixture was stirred for 80 h at 80 °C after which time it was filtered, the solid was extracted with copious amounts of chloroform, the organic layer was concentrated to give **3b** as a yellowish solid (0.27 g, 83%), m.p. >340 °C. ^{1}H NMR (500 MHz, $CDCl_3$, numbering as in Scheme 1): δ = 8.00 (d, J = 6 Hz, 4 H, H1, H4, H5, H8), 7.59 (d, J = 6.8 Hz, 2 H, H13, H20), 7.57 (d, J = 6.8 Hz, 2 H, H16, H23), 7.42 (d, J = 6.8 Hz, 4 H, H2, H3, H6, H7), 7.39 (t, J = 6 Hz, 2 H, H14, H21), 7.30 (t, J = 6.8 Hz, 2 H, H15, H22), 7.08 (s, 2 H, H12, H19), 3.94 (s, 4 H, 2× H17, 2× H24) ppm. ^{13}C NMR (125 MHz, $CDCl_3$): δ = 145.3 (C16a), 145.1 (C11), 143.8 (C12a), 133.5 (C12), 133.4 (C9), 129.7 (C8a), 126.7 (C14), 126.6 (C1), 125.3 (C2), 124.8 (C15), 123.7 (C16), 121.1 (C13), 44.5 (C17) ppm. $C_{32}H_{22}$ (406.53): calcd. C 94.55, H 5.45; found C 94.43, H, 5.50.

2,2′-Dimethyl-1,1′-biindenyl (*racemic*-9 and *meso*-9): To a stirred solution of 2-methylindene (0.8 mL, 6 mmol) in diethyl ether (6 mL) a solution of *n*BuLi (6.6 mmol) in hexanes was added and the reaction mixture was stirred for 1 h resulting in the formation of a pale yellow suspension which was added slowly to a cooled (–20 °C) suspension of cupric chloride (1 g, 7 mmol) in THF (10 mL). The resulting mixture was warmed to 5 °C and was stirred for one day, after which time it was quenched with methanol (5 mL), extracted with dichloromethane and separated (2–5% dichloromethane in cyclohexane) to give *meso*-**9** (310 mg, 40%), mixed fraction (152 mg, 19%), and *rac*-**9** (248 mg, 32%); *meso*-**9**: a yellow solid; m.p. 95–96 °C. ^{1}H NMR (500 MHz, $CDCl_3$, –15 °C, numbering as in Figure 7b): δ = 7.64 (d, J = 7 Hz, 1 H, H7), 7.36 (t, J = 7 Hz, 1 H, H5), 7.29 (t, J = 7 Hz, 1 H, H6), 7.29 (d, J = 7 Hz, 1 H, H4), 7.22 (d, J = 7 Hz, 1 H, H12), 7.13 (t, J = 7 Hz, 1 H, H13), 6.71 (t, J = 7 Hz, 1 H, H14), 6.60 (s, 1 H, H11), 6.28 (s, 1 H, H3), 5.88 (d, J = 7 Hz, 1 H, H15), 4.06 (s, 1 H, H9), 3.93 (s, 1 H, H1), 2.39 (s, 3 H, 3× H16), 1.59 (s, 3 H, 3× H8) ppm. ^{13}C NMR (125 MHz, $CDCl_3$): δ = 148.2 (C2), 147.1 (C10), 146.9 (C7a), 145.1 (C3a), 143.4 (C15a), 144.4 (C11a), 127.3 (C3), 128.1 (C11), 120.0 (C4), 126.9 (C5), 124.1 (C6), 122.6 (C7), 122.4 (C15), 123.6 (C14), 126.7 (C13), 119.9 (C12), 80.5 (C1), 53.7 (C9), 16.1 (C8), 16.0 (C16) ppm. $C_{20}H_{18}$ (258.36): calcd. C 92.98, H 7.02; found C 92.93, H 7.07; *racemic*-**9**: a yellow solid, m.p. 106–107 °C. ^{1}H NMR ofhe predominant (58%) conformer *rac*-**9b** (500 MHz, $CDCl_3$, –15 °C, numbering as in Figure 7a): δ = 7.12 (d, J = 7 Hz, 2 H, H4, H4′), 7.03 (t, J = 7 Hz, 2 H, H5, H5′), 6.94 (d, J = 7 Hz, 2 H, H7, H7′), 6.81 (t, J = 7 Hz, 2 H, H6, H6′), 6.68 (s, 2 H, 2 H, H3, H3′), 3.81 (s, 2 H, 2 H, H1, H1′), 2.41 (s, 6 H, 2× CH_3) ppm. ^{13}C NMR (125 MHz, $CDCl_3$): δ = 147.3 (C2), 143.2 (C7a), 144.7 (C3a), 128.7 (C3), 119.7 (C4), 126.6 (C5), 123.3 (C6), 122.2 (C7), 51.1 (C1), 16.0 (C8) ppm. $C_{20}H_{18}$ (258.36): calcd. C 92.98, H 7.02; found C 92.93, H 7.00.

9-Phenyl-11,12-bis(methoxycarbonyl)dibenzobarrelene (13): To a suspension of **2c** (203 mg, 0.8 mmol) in 1,4-dioxane (2 mL) dimethyl acetylenedicarboxylate (0.48 mL, 4 mmol) was added and the mixture was heated at 120 °C for 2 days after which time it was concentrated under ca. 1 mbar (to remove excess DMAD) and separated to give crude **13** (0.25 g, 79%) containing approx. 25% of the isomeric 1,4 adduct. Pure **13** was isolated by fractional crystallisation from acetone-hexane as a white solid: m.p. 158–159 °C. ^{1}H NMR (400 MHz, $CDCl_3$, numbering as in Figure 11): δ = 7.75 (d, J = 7.5 Hz, 2 H, H14, H18), 7.51 (t, J = 7.5 Hz, 2 H, H15, H17), 7.46 (t, J = 7.5 Hz, 1 H, H16), 7.42 (d, J = 7.5 Hz, 2 H, H1, H8), 7.10 (d, J = 7.5 Hz, 2 H, H4, H5), 7.03 (t, J = 7.5 Hz, 2 H,

H2, H7), 6.95 (t, J = 7.5 Hz, 2 H, H3, H6), 5.68 (s, 1 H, H10), 3.65 (s, 3 H, 3× H20), 3.77 (s, 3 H, 3× H19) ppm. ^{13}C NMR (100 MHz, $CDCl_3$): δ = 168.1 (C12a), 164.0 (C11a), 154.3 (C11), 144.6 (C12), 146.0 (C4a) 145.3 (C8a), 134.9 (C13), 130.4 (C14, C18), 128.3 (C15, C17), 127.6 (C16), 125.4 (C3), 124.8 (C2, C4), 123.7 (C1), 62.8 (C9), 52.4 (C19), 52.1 (C20), 51.4 (C10) ppm. MS (ES) 397 (31%, $[M + H]^+$). $C_{26}H_{20}O_4$ (396.44): calcd. C 78.77, H 5.09; found C 78.77, H 5.10.

Preparation of 9-(2-Indenyl)-11,12-bis(methoxycarbonyl)dibenzobarrelene (14): Analogously to **13**, **14** was prepared in a 21% yield as a white solid, m.p. 122 °C. ^{1}H NMR (400 MHz, $CDCl_3$, numbering as in Figure 11): δ = 7.59 (d, J = 7.5 Hz, 1 H, H18), 7.53 (d, J = 7.5 Hz, 1 H, H15), 7.47 (d, J = 7.5 Hz, 2 H, H4, H5), 7.42 (d, J = 7.5 Hz, 2 H, H1, H8), 7.37 (t, J = 7.5 Hz, 1 H, H16), 7.30 (t, J = 7.5 Hz, 1 H, H17), 7.09 (t, J = 7.5 Hz, 2 H, H2, H7), 7.03 (t, J = 7.5 Hz, 2 H, H3, H6), 5.71 (s, 1 H, H10), 3.94 (s, 2 H, 2× H19), 3.73 (s, 3 H, 3× H21), 3.72 (s, 3 H, 3× H20) ppm. ^{13}C NMR (100 MHz, $CDCl_3$): δ = 168.6 (C12a), 164.0 (C11a), 155.0 (C11), 141.6 (C12), 146.3 (C4a, C8b), 145.4 (C4b, C8a), 144.2 (C14a), 143.5 (C18a), 136.5 (C14), 127.0 (C16), 126.0 (C2, C7), 125.6 (C17), 125.4 (C3, C6), 124.4 (C4, C5), 124.3 (C1, C8), 123.9 (C18), 121.6 (C15), 61.3 (C9), 52.8 (C20, C21), 51.3 (C10) ppm. MS (ES) 433 (100%, $[M - H]^-$). $C_{29}H_{22}O_4$ (434.49): calcd. C 80.17, H 5.10; found C 80.11; H 4.99.

Preparation of 9-Phenyl-11,12-(*N*-methylpyrrolidiono)dibenzobarrelene (15): To a suspension of **2c** (25 mg, 0.1 mmol) in 1,4-dioxane (0.4 mL) *N*-methylmaleimide (25 mg, 0.22 mmol) was added and the mixture was heated at 120 °C for 1 day after which time it was cooled to give **15** (30 mg, 82%) as a white solid, m.p. 280–282 °C. ^{1}H NMR (500 MHz, $CDCl_3$, –15 °C, numbering as in Figure 14): δ = 8.10 (d, J = 8 Hz, 1 H, H18), 7.67 (m, 1 H, H17), 7.53 (m, 2 H, H15, H16), 7.45 (d, J = 7 Hz, 1 H, H5), 7.41 (m, 1 H, H14), 7.37 (d, J = 7 Hz, 1 H, H4), 7.29 (d, J = 7 Hz, 1 H, H1), 7.20 (t, J = 7 Hz, 2 H, H3, H6), 7.14 (t, J = 7 Hz, 1 H, H2), 7.05 (t, J = 7 Hz, 1 H, H7), 6.44 (d, J = 7 Hz, 1 H, H8), 4.86 (d, J = 3 Hz, 1 H, H10), 3.90 (d, J = 8.2 Hz, 1 H, H12), 3.30 (dd, J = 3, J = 8.2 Hz, 1 H, H11), 2.40 (s, 3 H, 3× H19) ppm. ^{13}C NMR (125 MHz, $CDCl_3$): δ = 177.0 (C11a), 175.0 (C12a), 144.8 (C8a), 140.7 (C8b), 140.2 (C4b), 138.0 (C4a), 135.3 (C13), 132.4 (C14), 129.8 (C18), 128.4 (C17), 127.6 (C16), 127.4 (C15), 127.2 (C3), 127.1 (C6), 126.7 (C2), 126.2 (C7), 125.4 (C8), 125.0 (C1,4), 123.5 (C5), 56.3 (C9), 49.1 (C11), 47.0 (C12), 46.2 (C10), 24.2 (C19) ppm. $C_{25}H_{19}NO_2$ (365.43): calcd. C 82.17, H 5.24, N 3.83; found C 81.87, H 5.25, N 3.85 (from chloroform).

Preparation of 1,6-Diphenyl-7,8,9,10-dibenzo-2,5-dioxabicyclo[4.2.2]-decane (20): To a suspension of the diol **18** (50 mg, 0.15 mmol) in toluene (6 mL) ethyleneglycol (0.15 mL) and *p*-toluenesulfonic acid (10 mg) were added and the mixture was heated at 60 °C for 3 h after which time it was separated (20% ethyl acetate in cyclohexane) to give **20** (30 mg, 52%) as a white solid, m.p. 229–231 °C. ^{1}H NMR (500 MHz, $CDCl_3$, numbering as in Figure 17): δ = 8.22 (d, J = 7.5 Hz, 2 H, H18, H24), 7.55 (t, J = 7.5 Hz, 2 H, H17, H23), 7.39 (t, J = 7.5 Hz, 2 H, H16, H22), 7.28 (t, J = 7.5 Hz, 2 H, H15, H21), 7.20 (dd, J = 9 Hz, 4 H, H2, H3, H6, H7), 6.93 (d, J = 7.5 Hz, 2 H, H14, H20), 6.85 (d, J = 9 Hz, 4 H, H1, H4, H5, H8), 3.47 (s, 4 H, 2× H11, 2× H12) ppm. ^{13}C NMR (125 MHz): δ = 145.1 (C13, C19), 141.7 (C4a, C4b, C8a, C8b), 129.6 (C14, C20), 129.2 (C1, C4, C5, C8), 128.5 (C2, C3, C6, C7), 127.6 (C15, C21), 127.5 (C17, C23), 127.2 (C18, C24), 127.1 (C16, C22), 79.2 (C9, C10), 67.5 (C11, C12) ppm. $C_{28}H_{24}O_2$ (392.50): calcd. C 85.68, H 6.16; found C 86.00, H 5.95.

X-Ray Measurements for 7, *anti*-3a, 3b, *rac*-9, *meso*-9, 10, 11, 13–20: Crystallographic data were collected using a Bruker SMART APEX CCD area detector diffractometer equipped with a Bruker SMART 1K CCD area detector and a rotating anode, using graphite-monochromated Mo-K_α radiation (λ = 0.71073 Å), and are

Table 2. Crystallographic data for *anti*-**3a**, **3b**, **7**, *rac*-**9** and *meso*-**9**.

Compound	*anti*-**3a**	**3b**	**7**	*rac*-**9**	*meso*-**9**
Empirical formula	$C_{32}H_{22}$	$C_{32}H_{22}$	$C_{23}H_{15}Br$	$C_{20}H_{18}$	$C_{20}H_{18}$
Formula weight	406.50	406.50	371.26	258.34	258.34
Crystal system	monoclinic	monoclinic	triclinic	monoclinic	triclinic
Space group	$P2_1/c$ (#14)	$P2_1/n$ (#14)	$P\bar{1}$ (#2)	$C2/c$ (#15)	$P\bar{1}$ (#2)
a /Å	12.2245(16)	6.7890(13)	6.8093(4)	19.672(2)	8.3004(5)
b /Å	8.0153(11)	9.1933(18)	10.8190(7)	5.4423(6)	10.1830(7)
c /Å	11.7765(16)	17.284(3)	11.9887(8)	15.2330(18)	18.7058(12)
α /deg	90	90	104.193(1)	90	96.752(1)
β /deg	113.182(3)	101.006(5)	105.234(1)	122.087(2)	99.324(1)
γ /deg	90	90	101.668(1)	90	111.291(1)
Volume /Å^3	1060.7(2)	1058.9(4)	791.87(9)	1381.7(3)	1426.69(16)
Z	2	2	2	4	4
Density (σ_{calc} /g cm^{-3})	1.273	1.275	1.557	1.242	1.203
Temperature /K	100(2)	100(2)	100(2)	100(2)	100(2)
Absorption coefficient (μ /mm^{-1})	0.072	0.072	2.595	0.070	0.068
F(000)	428	428	376	552	552
θ range /°	1.81–23.29	2.40–23.28	1.86–28.32	2.44–27.99	2.19–26.74
Index ranges	$-13 \le h \le 13$	$-7 \le h \le 7$	$-9 \le h \le 9$	$-25 \le h \le 25$	$-10 \le h \le 10$
	$-8 \le k \le 8$	$-10 \le k \le 10$	$-14 \le k \le 14$	$-7 \le k \le 7$	$-12 \le k \le 12$
	$-13 \le l \le 13$	$-19 \le l \le 19$	$-15 \le l \le 15$	$-20 \le l \le 20$	$-23 \le l \le 23$
Reflections measured	6899	6869	16306	6624	26052
Reflections used (R_{int})	1523 (0.0302)	1527 (0.0401)	3924 (0.0411)	1678 (0.0239)	6065 (0.0267)
Data/restraints/parameters	1523/0/145	1527/0/145	3924/0/277	1678/0/127	6065/0/505
Final R values $I > 2\sigma(I)$: R_1, wR_2	0.0385, 0.1015	0.0500, 0.1050	0.0319, 0.0772	0.0441, 0.1147	0.0400, 0.0967
R values (all data): R_1, wR_2	0.0515, 0.1086	0.0614, 0.1095	0.0367, 0.0792	0.0490, 0.1194	0.0457, 0.1003
Goodness-of-fit on F^2	1.067	1.146	1.044	1.061	1.025
Largest diff peak and hole /e Å^{-3}	0.226, –0.132	0.342, –0.168	0.600, –0.287	0.429, –0.217	0.287, –0.175

listed in Table 2, Table 3 and Table 4. A full sphere of the reciprocal space was scanned by phi-omega scans. A semi-empirical absorption correction, based on redundant reflections, was performed by the program SADABS.[26] The structures were solved by direct methods and refined by full-matrix least-squares on F^2 for all data using the program library SHELXTL.[27,28] Hydrogen atom treatment varied from compound to compound, depending on the crystal quality. In **7**, *meso*-**9**, *rac*-**9**, **14**, and **17**–**21** all hydrogen atoms were located in the difference Fourier map and allowed to refine freely. In **3a**, **3b**, **10**, **11**, **15** and **16** all hydrogen atoms were added

Table 3. Crystallographic data for **10**, **11**, **13**, **14** and **15**.

Compound	**10**	**11**	**13**	**14**	**15**
Empirical formula	$C_{26}H_{18}$	$C_{20}H_{10}F_4$	$C_{26}H_{20}O_4$	$C_{29}H_{22}O_4$	$C_{25}H_{19}NO_2$
Formula weight	330.4	326.28	396.42	434.47	365.41
Crystal system	orthorhombic	orthorhombic	triclinic	triclinic	monoclinic
Space group	*Pbca* (#61)	$P2_12_12_1$ (#19)	$P\bar{1}$ (#2)	$P\bar{1}$ (#2)	$P2_1$ (#4)
a /Å	8.379(2)	10.7580(12)	8.0579(12)	8.1407(10)	12.9175(12)
b /Å	19.994(5)	12.5118(14)	10.5738(16)	15.5856(19)	7.8430(8)
c /Å	20.615(5)	21.704(2)	11.9703(19)	18.628(2)	17.9211(17)
α /deg	90	90	79.394(3)	66.062(3)	90
β /deg	90	90	84.371(3)	83.831(3)	91.152(2)
γ /deg	90	90	74.707(3)	86.388(3)	90
Volume /Å^3	3445.1(15)	2921.3(6)	965.7(3)	2147.2(4)	1815.3(3)
Z	8	8	2	4	4
Density (σ_{calc} /g cm^{-3})	1.274	1.484	1.363	1.344	1.337
Temperature /K	100(2)	100(2)	100(2)	100(2)	293(2)
Absorption coefficient (μ /mm^{-1})	0.072	0.121	0.091	0.089	0.085
F(000)	1392	1328	416	912	768
θ range /°	1.98–23.35	1.88–26.37	1.73–26.44	1.43–23.28	1.14–26.43
Index ranges	$-9 \le h \le 8$	$-13 \le h \le 13$	$-10 \le h \le 10$	$-9 \le h \le 9$	$-16 \le h \le 16$
	$-22 \le k \le 22$	$-15 \le k \le 15$	$-13 \le k \le 13$	$-17 \le k \le 17$	$-9 \le k \le 9$
	$-21 \le l \le 22$	$-27 \le l \le 27$	$-14 \le l \le 14$	$-20 \le l \le 20$	$-22 \le l \le 22$
Reflections measured	14419	25884	17283	14609	16191
Reflections used (R_{int})	2454 (0.0588)	3353 (0.0300)	3957 (0.0305)	6107 (0.0286)	4000 (0.0292)
Data/restraints/parameters	2454/0/235	3353/40/518	3957/0/351	6107/0/599	4000/1/507
Final *R* values $I > 2\sigma(I)$: R_1, wR_2	0.0593, 0.1505	0.0569, 0.1477	0.0355, 0.0863	0.0610, 0.1613	0.0363, 0.0885
R values (all data): R_1, wR_2	0.0757, 0.1662	0.0601, 0.1511	0.0416, 0.0902	0.0694, 0.1663	0.0405, 0.0907
Goodness-of-fit on F^2	1.023	1.081	1.038	1.065	1.031
Largest diff peak and hole /e Å^{-3}	0.482, –0.252	0.654, –0.215	0.313, –0.203	0.400, –0.251	0.160, –0.224

Table 4. Crystallographic data for **16**, **17**, **18**, **19** and **20**.

Compound	**16**	**17**	**18**	**19**	**20**
Empirical formula	$C_{28}H_{22}$	$C_{28}H_{24}O$	$C_{26}H_{20}O_2$	$C_{28}H_{24}O_2$	$C_{28}H_{22}O_2$
Formula weight	358.46	376.47	364.42	392.47	390.46
Crystal system	monoclinic	triclinic	triclinic	triclinic	monoclinic
Space group	$P2_1/c$ (#14)	$P\bar{1}$ (#2)	$P\bar{1}$ (#2)	$P\bar{1}$ (#2)	$C2/c$ (#15)
a /Å	20.3035(14)	9.6559(8)	6.7449(10)	7.0964(5)	22.0418(16)
b /Å	18.5851(13)	10.5285(8)	8.0370(11)	8.9046(7)	8.5713(6)
c /Å	9.8377(7)	10.6096(9)	8.9216(13)	8.9274(7)	21.1386(15)
α /deg	90	88.107(2)	102.967(3)	104.086(2)	90
β /deg	90.085(2)	72.505(1)	96.351(3)	95.407(2)	92.319(1)
γ /deg	90	74.525(1)	106.587(3)	113.174(1)	90
volume /Å^3	3712.2(5)	990.10(14)	443.71(11)	491.46(6)	3990.4(5)
Z	8	2	1	1	8
Density (σ_{calc} /g cm^{-3})	1.283	1.263	1.364	1.326	1.300
Temperature /K	100(2)	100(2)	100(2)	100(2)	100(2)
Absorption coefficient (μ /mm^{-1})	0.072	0.075	0.085	0.082	0.080
F(000)	1520	400	192	208	1648
θ range /°	1.10–23.32	2.01–26.00	2.38–30.47	2.41–31.98	1.85–28.31
Index ranges	$-22 \le h \le 22$	$-11 \le h \le 11$	$-9 \le h \le 9$	$-10 \le h \le 10$	$-29 \le h \le 29$
	$-20 \le k \le 20$	$-12 \le k \le 12$	$-11 \le k \le 11$	$-13 \le k \le 12$	$-11 \le k \le 11$
	$-8 \le l \le 10$	$-13 \le l \le 13$	$-12 \le l \le 12$	$-13 \le l \le 13$	$-27 \le l \le 28$
Reflections measured	18062	17084	10310	12003	19710
Reflections used (R_{int})	5355 (0.0268)	3886 (0.0207)	2661 (0.0258)	3203 (0.0242)	4958 (0.0254)
Data/restraints/parameters	5355/0/506	3886/0/358	2661/0/167	3203/0/184	4928/0/362
Final *R* values $I > 2\sigma(I)$: R_1, wR_2	0.0337, 0.0822	0.0375, 0.0942	0.0472, 0.1295	0.0479, 0.1310	0.0445, 0.1145
R values (all data): R_1, wR_2	0.0413, 0.0862	0.0400, 0.0961	0.0538, 0.1353	0.0547, 0.1369	0.0514, 0.1194
Goodness-of-fit on F^2	1.035	1.033	1.037	1.036	1.027
Largest diff peak and hole /e Å^{-3}	0.196, –0.161	0.351, –0.220	0.541, –0.209	0.553, –0.163	0.424, –0.200

at calculated positions and refined using a riding model. Their isotropic temperature factors were fixed to 1.2 times the equivalent isotropic displacement parameters of the carbon atom to which the H-atom is attached.

CCDC-756592 (for **7**), -756591 (for *anti*-**3a**), -756588 (for **3b**), -756593 (for *rac*-**9**), -756590 (for *meso*-**9**), -756595 (for **10**), -756586 (for **11**), -756596 (for **13**), -756587 (for **14**), -756599 (for **15**), -756600 (for **16**), -756598 (for **17**), -756589 (for **18**), -756597 (for **19**), -756594 (for **20**) contain the supplementary X-ray crystallographic data for this paper. These data can be obtained free of charge from The Cambridge Crystallographic Data Centre via www.ccdc.cam.ac.uk/data_request/cif.

Acknowledgments

We thank Science Foundation Ireland and University College Dublin for generous financial support, and Dr. J. Muldoon for the 2D EXSY data on molecule **20**.

[1] a) V. Pophristic, L. Goodman, *Nature* **2001**, *411*, 565; b) M. Oki, *Top. Stereochem.* **1983**, *14*, 1–81; c) S. Brydges, L. E. Harrington, M. J. McGlinchey, *Coord. Chem. Rev.* **2002**, *233/234*, 75–105.

[2] a) M. J. Hafezi, F. J. Sharif, *THEOCHEM* **2008**, *814*, 43–49; b) J. R. Durig, D. A. C. Compton, *J. Phys. Chem.* **1979**, *83*, 265–268.

[3] a) M. Nakamura, M. Oki, *Bull. Chem. Soc. Jpn.* **1975**, *48*, 2106–2111; b) M. Oki, I. Fujino, D. Kawaguchi, K. Chuda, Y. Moritaka, Y. Yamamoto, S. Tsuda, T. Akinaga, M. Aki, H. Kojima, N. Morita, M. Sakurai, S. Toyota, Y. Tanaka, T. Tanuma, G. Yamamoto, *Bull. Chem. Soc. Jpn.* **1997**, *70*, 457–469; c) G. Yamamoto, M. Suzuki, M. Oki, *Angew. Chem.* **1981**, *93*, 580–581; *Angew. Chem. Int. Ed. Engl.* **1981**, *20*, 607–608; d) D. Zehm, W. Fudickar, M. Hans, U. Schilde, A. Kelling, T. Linker, *Chem. Eur. J.* **2008**, *14*, 11429–11441; e) A. Caspar, S. Altenburger-Combrisson, F. Gobert, *Org. Magn. Reson.* **1978**, *11*, 603–606; f) P. J. Marriott, Y.-H. Lai, *J. Chromatogr.* **1988**, *447*, 29–41.

[4] a) K. M. Mislow, *Introduction to Stereochemistry*, W. A. Benjamin, Inc., **1965**, pp. 78–79; b) G. H. Christie, J. J. Kenner, *J. Chem. Soc.* **1922**, *121*, 614–620; c) R. Adams, H. C. Yuan, *Chem. Rev.* **1933**, *12*, 261–338; d) G. Yamamoto, T. Nemoto, Y. Ohashi, *Bull. Chem. Soc. Jpn.* **1992**, *65*, 1957–1966; e) A. Mazzanti, L. Lunazzi, M. Minzoni, J. E. Anderson, *J. Org. Chem.* **2006**, *71*, 5474–5481; f) G. Bringmann, A. J. P. Mortimer, P. A. Keller, M. J. Gresser, J. Garner, M. Breuning, *Angew. Chem.* **2005**, *117*, 5518–5563; *Angew. Chem. Int. Ed.* **2005**, *44*, 5384–5427.

[5] a) T. R. Kelly, M. C. Bowyer, K. V. Bhaskar, D. Bebbington, A. Garcia, F. Lang, M. H. Kim, M. P. Jette, *J. Am. Chem. Soc.* **1994**, *116*, 3657–3658; b) T. R. Kelly, J. P. Sestelo, I. N. Tellitu, *J. Org. Chem.* **1998**, *63*, 3655–3665; c) T. R. Kelly, *Acc. Chem. Res.* **2001**, *34*, 514–522; d) M. Llunell, P. Alemany, J. M. Bofill, *ChemPhysChem* **2008**, *9*, 1117–1119; e) T. F. Magnera, J. Michl, *Top. Curr. Chem.* **2005**, *262*, 63–97, and references cited therein; f) I. Yoon, D. Bentez, Y.-L. Zhao, O. Miljanic, S.-Y. Kim, E. Tkatchouk, K. C.-F. Leung, S. I. Khan, W. A. Goddard, J. F. Stoddart, *Chem. Eur. J.* **2009**, *15*, 1115–1122; g) R. D. Rasberry, K. D. Shimizu, *Org. Biomol. Chem.* **2009**, *7*, 3899–3905; h) V. Serreli, C.-F. Lee, E. R. Kay, D. A. Leigh, *Nature* **2007**, *445*, 523–527; i) J. Hernandez, E. R. Kay, D. A. Leigh, *Science* **2004**, *306*, 1532–1537; j) G. S. Kottas, L. I. Clarke, D. Horinek, J. Michl, *Chem. Rev.* **2005**, *105*, 1281–1376.

[6] a) H. Iwamura, K. Mislow, *Acc. Chem. Res.* **1988**, *21*, 175–182; b) T. R. Kelly, R. A. Silva, H. De Silva, S. Jasmin, Y. Zhao, *J. Am. Chem. Soc.* **2000**, *122*, 6935–6949; c) L. Grill, K.-H. Rieder, F. Moresco, G. Rapenne, S. Stojkovic, X. Bouju, C. Joachim, *Nat. Nanotechnol.* **2007**, *2*, 95–98.

[7] a) T. A. Albright, P. Hofmann, R. Hoffmann, C. P. Lillya, P. A. Dobosh, *J. Am. Chem. Soc.* **1983**, *105*, 3396–3411; b) Y. F. Oprunenko, *Russ. Chem. Rev.* **2000**, *69*, 683–704; c) S. Brydges, N. Reginato, L. P. Cuffe, C. M. Seward, M. J. McGlinchey, *C. R. Chim.* **2005**, *8*, 1497–1505; d) E. Kirillov, S. Kahlal, T. Roisnel, T. Georgelin, J.-Y. Saillard, J. F. Carpentier, *Organometallics* **2008**, *27*, 387–393; e) G. Yamamoto, *Pure Appl. Chem.* **1990**, *62*, 569–574.

[8] a) L. E. Harrington, L. S. Cahill, M. J. McGlinchey, *Organometallics* **2004**, *23*, 2884–2891; b) K. Nikitin, H. Müller-Bunz, Y. Ortin, M. J. McGlinchey, *Org. Biomol. Chem.* **2007**, *5*, 1952–1960.

[9] a) H. Förster, F. Vögtle, *Angew. Chem.* **1977**, *89*, 443–455; *Angew. Chem. Int. Ed. Engl.* **1977**, *16*, 429–441; b) G. Bott, L. D. Field, S. Sternhell, *J. Am. Chem. Soc.* **1980**, *102*, 5618–5626; c) L. Lunazzi, A. Mazzanti, M. Minzoni, *J. Org. Chem.* **2006**, *71*, 9297–9301; d) R. Ruzziconi, S. Spizzichino, L. Lunazzi, A. Mazzanti, M. Schlosser, *Chem. Eur. J.* **2009**, *15*, 2645–2652.

[10] K. Nikitin, H. Müller-Bunz, Y. Ortin, M. J. McGlinchey, *Chem. Eur. J.* **2009**, *15*, 1836–1843.

[11] As emphasised by Sternhell[9b] the geometric parameters, such as CAD or *r** have been introduced merely as a convenient measure of the severity of non-bonded interactions and give no insight into the actual details of geometry of the transition state.

[12] D.-W. Lee, J. Yun, *Bull. Korean Chem. Soc.* **2004**, *25*, 29–30.

[13] H. Dang, M. A. Garcia-Garibay, *J. Am. Chem. Soc.* **2001**, *123*, 355–356.

[14] K. Nikitin, H. Müller-Bunz, Y. Ortin, W. Risse, M. J. McGlinchey, *Eur. J. Org. Chem.* **2008**, 3079–3084.

[15] N. M. Sergeyev, K. F. Abdulla, V. R. Skvarchenko, *J. Chem. Soc., Chem. Commun.* **1972**, 368–370.

[16] J. P. N. Brewer, I. F. Eckhard, H. Heaney, B. A. Marples, *J. Chem. Soc. C* **1968**, 664–676.

[17] J. Trotter, F. C. Wireko, *Acta Crystallogr., Sect. C* **1991**, *47*, 1275–1277.

[18] L. R. C. Barclay, R. A. Chapman, *Can. J. Chem.* **1965**, *43*, 1754–1760.

[19] W. J. Wasserman, M. C. Kloetzel, *J. Am. Chem. Soc.* **1953**, *75*, 3036–3038.

[20] P. Reutenauer, P. J. Boul, J.-M. Lehn, *Eur. J. Org. Chem.* **2009**, 1691–1697.

[21] C. Pinazzi, *Ann. Chim.* **1962**, *7*, 397–408.

[22] J. L. Cook, C. A. Hunter, C. M. R. Low, A. Perez-Velasco, J. G. Vinter, *Angew. Chem.* **2007**, *119*, 3780–3783; *Angew. Chem. Int. Ed.* **2007**, *46*, 3706–3709.

[23] D. B. Li, W. F. Paxton, R. H. Baughman, T. J. Huang, J. F. Stoddart, P. S. Weiss, *MRS Bull.* **2009**, *34*, 671–681, and references cited therein.

[24] H. S. Gutowsky, C. H. Holm, *J. Chem. Phys.* **1956**, *25*, 1228–1234.

[25] B. H. Klandermann, T. R. Criswell, *J. Org. Chem.* **1969**, *34*, 3426–3430.

[26] G. M. Sheldrick, *SADABS*, Bruker AXS Inc., Madison, WI 53711, **2000**.

[27] G. M. Sheldrick, *SHELXS-97*, University of Göttingen, Germany, **1997**.

[28] G. M. Sheldrick, *SHELXL-97-2*, University of Göttingen, Germany, **1997**.

Received: June 13, 2010
Published Online: August 16, 2010

